Self-supported yttria-stabilized zirconia mesocrystals with tunable mesopores prepared by a chemi-thermal process

Liu, Leifeng; Eriksson, Mirva; Zou, Ji; Zhong, Yuan; Liu, Qi; Liu, Zhi; Chiu, Yu Lung; Shen, Zhijian

DOI:
10.1016/j.jmat.2019.03.001

Journal of Materiomics 5 (2019) 350–356

Contents lists available at ScienceDirect

Journal of Materiomics

journal homepage: www.journals.elsevier.com/journal-of-materiomics/

Self-supported yttria-stabilized zirconia mesocrystals with tunable mesopores prepared by a chemi-thermal process

Leifeng Liu [a, b, c], Mirva Eriksson [a], Ji Zou [b], Yuan Zhong [a], Qi Liu [d], Zhi Liu [d], Yu-Lung Chiu [b], Zhijian Shen [a, *]

[a] Department of Materials and Environmental Chemistry, Arrhenius Laboratory, Stockholm University, 10691, Stockholm, Sweden
[b] School of Metallurgy and Materials, University of Birmingham, B15 2TT, UK
[c] Department of Materials Science and Engineering, South University of Science and Technology of China, 518055, China
[d] Size Materials Co., Jiujiang, China

ARTICLE INFO

Article history:
Received 20 January 2019
Received in revised form
5 March 2019
Accepted 10 March 2019
Available online 13 March 2019

Keywords:
Mesocrystal
Mesoporous
Yttria-stabilized zirconia
Industry production

ABSTRACT

Mesoporous mesocrystals are highly desired in catalysis, energy storage, medical and many other applications, but most of synthesis strategies involve the usage of costly chemicals and complicated synthesis routes, which impede the commercialization of such materials. During the sintering of dense ceramics, coarsening is an undesirable phenomenon which causes the growth of the grains as well as the pores hence hinders the densification, however, coarsening is desired in the sintering of porous ceramics to expand the pore sizes while retaining the total pore volume. Here we report a chemi-thermal process, during which nanocrystallite aggregates were synthesized by hydrothermal process and then converted to the product by sintering. Through this strategy, we synthesized mesoporous self-supported mesocrystals of yttria-stabilized zirconia with tunable pore size and the process was then scaled-up to industrial production. The thermal conductivity measurement shows that the mesoporous powder is a good thermal isolator. The monolith pellets can be obtained by SPS sintering under high pressure and the mesoporosity is retained in the monolith pellets. This work features facile and scalable process as well as low cost raw chemicals making it highly desirable in industrial applications.

1. Introduction

Mesopores can be introduced into self-supported mesocrystal particles resulting in a kind of materials highly desired in catalysis, energy storage, medical and many other applications since they possess advantages provided both by nano-particles and relatively larger single crystals [1–5]. On one hand, similar to nano-crystals, they show large surface area for adsorption and catalysis reactions; on the other hand, self-supported mesocrystals are easy to handle in industrial production process as well as show certain degree of structural coherence hence good mechanical stability [3,6,7]. Currently, there are mainly two approaches to synthesis self-supported mesoporous mesocrystals and mesoporous single crystals: (1) by using hard template: e.g. Edward and et al. used nano silica particles as the hard template to synthesize mesoporous TiO_2 single crystals which show high electronic mobility [6]; (2) by using soft surfactants: e.g. Yong L. and et al. used Pluronic P123 to direct the formation of TiO_2 mesocrystals by hydrothermal reaction [8–10]. Both of these two approaches involve the using of costly chemicals, which impedes the large scale industrial production and application.

Nanocrystallite aggregates can be obtained as the product from the hydrothermal synthesis of some inorganic oxides e.g. zeolites, ZnO_2 and TiO_2 [11–14]. A considerable amount of intercrystal pores are normally presented in such powders due to imperfect stacking of nanocrystallites [11,14]. However, such kind of structures is fragile due to the loose bonding between nanocrystals [15,16]. Moreover, the obtained pore size may not match the requirement of the application.

Sintering is a process conventionally used to convert porous green bodies into dense ceramics. Similar to a ceramic green body, each nanocrystallite aggregate is an assembling of thousands of crystallites, hence heat treatment of the powder is a sintering process for each particle. During the sintering process, different

* Corresponding author.
E-mail address: shen@mmk.su.se (Z. Shen).
Peer review under responsibility of The Chinese Ceramic Society.

https://doi.org/10.1016/j.jmat.2019.03.001

mass transportation mechanisms are divided into two competing categories resulting either coarsening or densification effect. Although sintering is normally employed to eliminate the pores, porous ceramics with various pore sizes can be achieved when coarsening mechanisms outweigh densification mechanisms during sintering [16–18]. Therefore instead of densifying the nanocrystallite aggregates, sintering process can possibly be used to adjust the pore size when coarsening mechanisms overweigh densification mechanisms. Moreover, sintering can also enhance the bonding between the nanocrystallites thus to improve the mechanical stability of the structure which is a crucial but often absent properties for the application of mesoporous materials [19].

In this work, yttria-stabilized zirconia (YSZ) self-supported mesocrystals with tunable pore sizes were synthesized through a chemi-thermal process. The nanocrystallite aggregates of YSZ were firstly obtained through hydrothermal synthesis. Then sintering of the obtained nanocrystallite aggregates produce mesoporous YSZ with tunable pore size. In the as-hydrothermal synthesized nanocrystallite aggregates the crystallites are roughly aligned and in the size of a few nanometers, which causes coarsening mechanisms, especially coalescence, to dominate the sintering process leading to the formation of mesoporous YSZ self-supported mesocrystals. In additional, monolith pellets with retained mesoporosity are also fabricated at 450 °C under 120 MPa applied pressure by spark plasma sintering (SPS). This chemi-thermal process is facile and scalable and uses only low cost raw chemicals, which makes it highly desirable in industrial applications as catalyst support, bioceramics, electrolyte and so on [20,21]. As an example of the potential applications, we show that the mesoporous YSZ is an excellent thermal insulator with considerably lower thermal conductivity than the macroporous counterpart [22–25]. This work paves the way to a top-down synthesis strategy of mesoporous inorganic materials.

2. Materials and methods

2.1. Materials and sample preparation

Synthesis of YSZ nanocrystallite aggregates and the sintering process. Solution A: 20 mmol of $ZrOCl_2 \cdot 8H_2O$ was dissolved in 50 ml of deionized H_2O; Solution B: 0.6 mmol of YCl_3 was dissolved in 10 ml H_2O; The two solutions were then mixed together and 2 M NH_3OH solution was added drop-wise under vigorous stirring to the mixed solution till PH = 6. The gel obtained was transferred to an autoclave of 200 ml for the hydrothermal treatment at 190 °C for 10 h. The product was washed with excess water and ethanol. Then the product was dried at 200 °C in air. The sintering was carried out in a muffle furnace in air atmosphere at the temperature of 300, 450, 500, 550, 600 700 and 900 °C. The corresponding product is denoted by the sintering temperature as S300, S450, S500, S550, S600, S700 and S900.

The fabrication of monolith. 2 g of as-synthesized YSZ powder was firstly dried in vacuum at 200 °C for 2 h before loaded into a graphite die of 12 mm in diameter. The sintering is carried out in a spark plasma sintering (SPS) furnace (Dr Sinter, SPS-825, Fuji Electronics, Japan). The sintering temperature is measured through a thermal couple in contact with the die. The sample was heated up at the rate of 100 °C per minute to 450 °C and held for 5 min before the sample was furnace cooled to room temperature. A pressure of 120 MPa was applied to the sample at 450 °C and kept to the end of the sintering. The obtained monolith sintered aggregate sample is denoted as SPS450.

2.2. Characterization

SEM observation was carried out on JEOL JSM-7401 F equipped with cold field emission gun and TEM observation was carried out on a JEOL JEM-2100 LaB_6 microscope operating at 200 kV. To prepare the sample for electron tomography, YSZ powder after sintering at 700 °C was dispersed in ethanol solution which was then deposit onto the copper TEM grid (with carbon film). A droplet of a colloidal gold solution with gold particle size of 5 nm was then deposit on the gird to serve as the markers during the data reconstruction process. A tilt series of 51 TEM images with tilt step of 2° were collected to cover the range of 102°. The reconstruction was done by using software kit IMOD. N_2 adsorption-desorption isotherm was measured at 77 K by using a Micromeritics ASAP2020 analyzer. The pore distribution and pore volume were analyzed by BJH method. Powder X-ray diffraction (PXRD) patterns were collected on a Panalytical X'Pert PRO diffractometer operating in reflection mode. The Rietveld refinement of the PXRD patterns was done by using software suite TOPAS-Academic. To measure the thermal diffusivity, as-synthesized powder was mixed with binder solution in a weight ratio of 9:1 and then pressed into pellets of 10 mm in diameter by using a uniaxial hydraulic press. Thermal diffusivity was measured by laser flash method at room temperature using a Netzsch LFA 427 machine.

3. Results and discussion

The as-synthesized YSZ powder consists of compressed globular particles of around 100 nm in diameter (Fig. 1a) and each particle is an aggregate of nanocrystallites of 3–5 nm in size. The corresponding SAED pattern shows broadened diffraction spots instead of ring pattern implying that the nanocrystals in the particle are aligned along similar crystallographic direction. The assembling of nanocrystallites takes place presumably during the hydrothermal process.

Sintering at 450 °C causes slightly growth of the nanocrystallites, however the diffraction pattern is still similar to the one obtained from as-synthesized sample. After sintered at 700 °C, both the sizes of nanocrystallites and the pores increase to around 10–20 nm in diameter. It is also noticed that the broadened diffraction spots become a few sets of slightly misorientated diffraction patterns with sharp spots, which indicates that the nanocrystallites within each particle are grouped into a few single crystals with small misorientations among them, which is a typical feature of the mesocrystal materials [2]. Increase sintering temperature to 900 °C causes the further growth of the crystals and the interconnected pores become isolated.

Fig. 2a shows a HR-TEM image taken on a particle from S700 sample. We did FFT on the marked area to study the orientation difference. It was found that all the marked areas are along [001] direction (Fig. 2b), implying that after sintering at 700 °C the nanocrystallite aggregates become particles of self-supported porous structure composed of well aligned and connected nanocrystallites.

The synthesis of YSZ powder was also scaled up by using a 1200 L hydrothermal reactor in the factory of Size Materials Co., Jiujiang, China. The recipe of the industrial scale production is similar but not strictly the same as the lab one. 96.5 Kg of powder can be obtained from each batch and the yield was over 95%. The same microstructure as in the lab synthesized YSZ can be obtained. The facile synthesis procedure makes the scale-up process straight forward, which is not achieved in most of the other published method for the synthesis of mesoporous mesocrystal materials. The

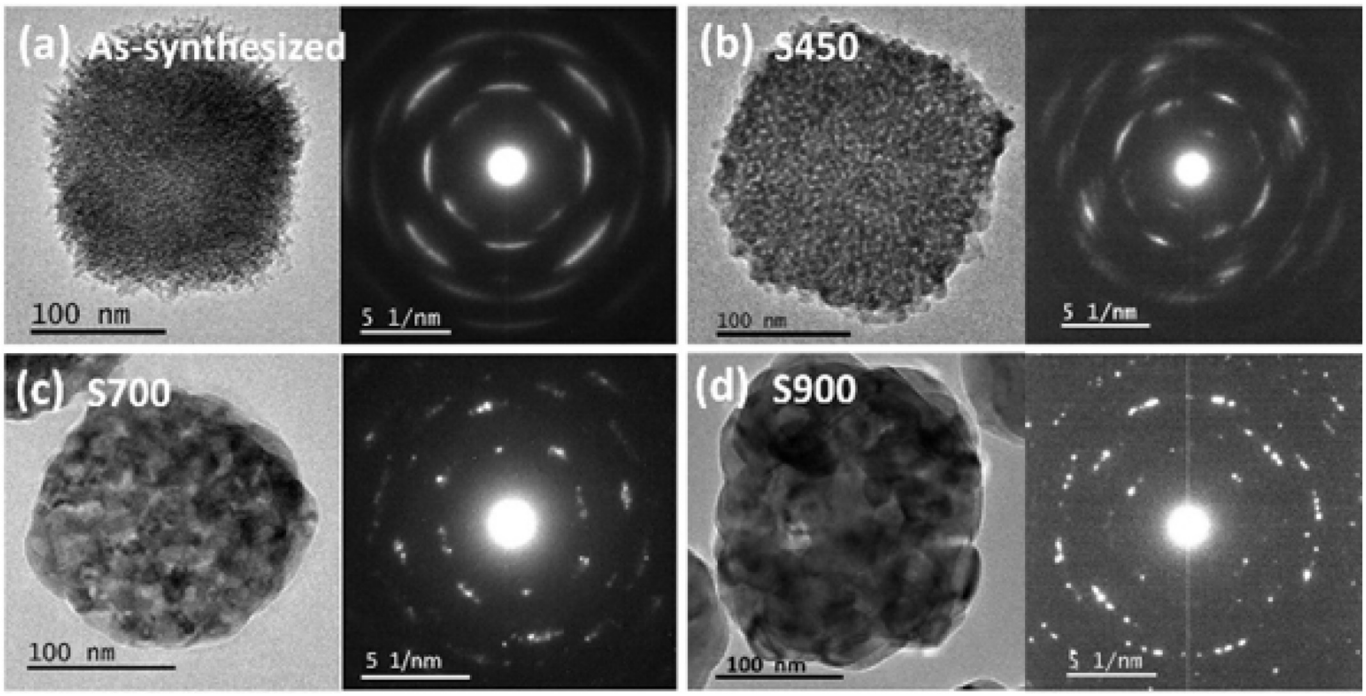

Fig. 1. The arrangement and the size of the nanocrystallites as well as the morphology of the particles after sintered at different temperature. (a-d) TEM images and the corresponding selected area electron diffraction (SAED) patterns of the as-synthesized sample, S450, S700 and S900.

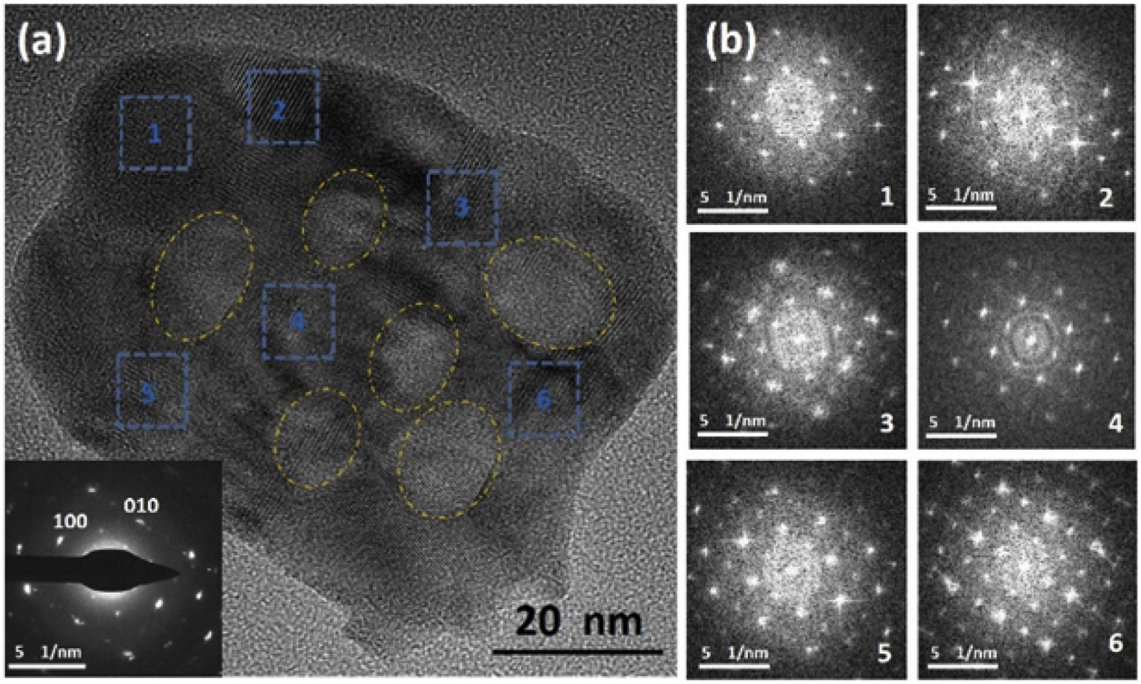

Fig. 2. Nanocrystallites are well aligned in the mesoporous YSZ mesocrystal particle after sintered at 700 °C. (a) High resolution TEM (HR-TEM) image and the SAED pattern (insert) of a particle from sample S700. Pores are indicated by yellow ellipses. (b) The fast Fourier transform (FFT) of the marked areas (blue square) in the HRTEM image.

industrial scale production of this material also makes it possible for other researchers to look for the applications of this material and test it in real-life scale.

Since TEM images are the projections of an object along particular directions, the lacking of 3-dimensional information could lead to misinterpretation of the images, for instance, particles with homogeneously distributed pores or with pores just on the surface gives out similar contrast in TEM images [26]. Therefore in

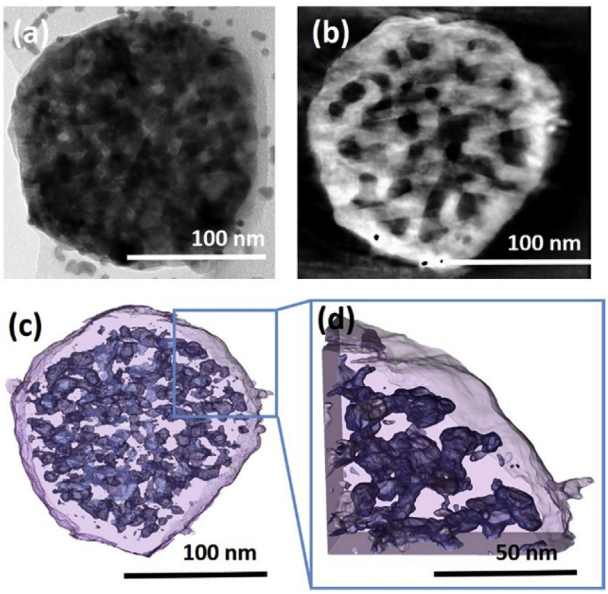

Fig. 3. (a) TEM image of a mesoporous YSZ mesocrystal particle from the sample after sintered at 700 °C(S700), (b) a slice of the electron tomography of the particle and (c, d) 3D model of a part (thickness: 40 nm) of the particle.

this work the distribution of the pores was studied by electron tomography technic which uses a tilt series of TEM images to reconstruct the 3D model of a particle. Fig. 3a shows the TEM image of a particle after sintered at 700 °C. The black dots in the image are nano gold particles added to the sample as the markers to align the tile series of images for the reconstruction of the tomography. The pores in the particle can be seen from the variation of the contrast in the TEM image but the size and distribution are still hardly resolved. Fig. 3b shows a slice of the reconstructed tomography from the middle part of the particle. It is clearly resolved that the pores are in the size of around 10 nm, which is in a good agreement with the result from N_2 isothermal presented below. It is also revealed that the pores are connected and homogeneously distributed in the particle (Fig. 3c and d and video 1).

Supplementary video related to this article can be found at https://doi.org/10.1016/j.jmat.2019.03.001

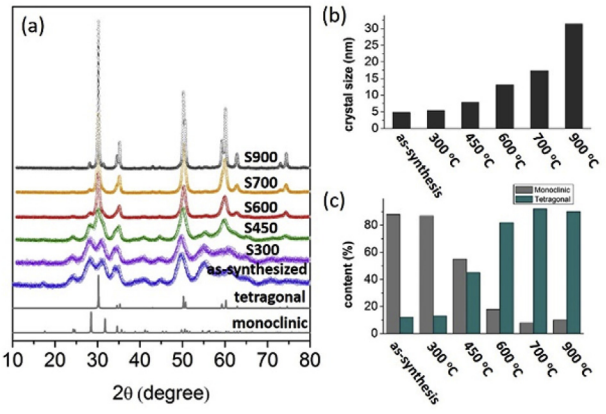

Fig. 4. (a) PXRD patterns of the mesoporous YSZ mesocrystal powders sintered at different temperature and the simulated reference patterns of the monoclinic and tetragonal ZrO_2. b) and c) The crystal sizes and phase ratio obtained from Rietveld refinement of the powder XRD patterns.

PXRD patterns (Fig. 4a) were collected and Rietveld refinement were performed to study the crystallite size and phase ratio (between monoclinic and tetragonal) in the samples. The crystallite size increases gradually from around 5 nm for the as-synthesized powder to around 17.5 nm and 31 nm for the S700 and S900 powder (Fig. 4b). Fig. 4c shows that the as-synthesized powder composed mainly by monoclinic phase and the ratio of tetragonal phase increases as the increase of sintering temperature. This is due to the stability of the tetragonal phase YSZ increases as the increase of the crystallite sizes. The high sintering temperature overcame the energy barrier to convert metastable monoclinic phase obtained from the hydrothermal process to tetragonal phase.

The porosity of the YSZ powders was further analyzed by using N_2 adsorption-desorption isothermal (Fig. 5). The as-synthesized powder shows high adsorption of N_2 at low relative pressure region which indicates the existence of considerable amount of micropores (pore size < 2 nm). For the sintered samples the intake of N_2 at low pressure region drops sharply while the hysteresis loop becomes more pronounced implying the disappearing of the micropores and the appearing of the mesopores (2 nm < pore size < 50 nm). It can also be noticed that the hysteresis loop moves toward higher relative pressure region as the increase of the heating temperature, which implies the increase of the pore size. Fig. 5b shows the pore size distribution by plotting the incremental pore volume against the pore width. The as-synthesized powder contains mainly micropores and the increase of the sintering temperature caused gradual increase of the pore size from around 3.3 nm (S450) to 10.5 nm (S700). However, after sintering at 900 °C, negligible amount of pores is observed implying the collapse of the mesoporous structure. The N_2 adsorption data confirms the TEM analysis results that the mesopores were generated after sintering of the as-synthesized microporous YSZ powder. More importantly, it shows that the size of the pores can be rationally controlled by adjusting the sintering temperature.

Fig. 5c shows the changes of the pore volume of the pores in size between 1.5 nm and 15 nm and the BET surface area. As expected, both of them decreases as the increase of sintering temperature. However it is found that the BET surface area drops gradually over the temperature range while the pore volume shows sharp drop after sintering at 600 °C and 900 °C. The decrease of the BET surface area was due to the growth of the nanocrystallites which occurred continuously with the increase of the sintering temperature. In contrast, the pore volume was not affected by the crystallite growth. While two possible reasons can lead to the decrease of the pore volume: 1) the shrink of the particles can results in the shrink of pores; 2) the connectivity of the pores decrease as the growth of crystals and the increase of the pore size. As a result, some of the pores become closed pores. A study from Coleman and Beere shows that the volume of closed pore starts to increase when the porosity decreases to 15% during the sintering of a homogeneously packed UO_2 ceramic [27]. In this work, each particle in the as-synthesized powder is an assembling of around a few thousands of aligned nanocrystals. Therefore the heat treatment process is a sintering process for each particle. If the pores between 1.5 nm and 15 nm are assumed to be mainly the intra-granule pores, the open porosity of the particles can be calculated to be around 31% for as-synthesized sample and 18% for S700 sample, which implies that the porosity is still too high for the formation of closed pores at this stage. Hence the decrease of the pore volume in the samples sintered at and below 700 °C was due to the shrinkage of the particles. This is also supported by the tomography results of the 700 °C sintered powder, as the pores are still forming well connected network. While the sudden drop of the pore volume after 900 °C sintering can be attributed to both of the two mechanisms.

Sintering is a competition process between densification and

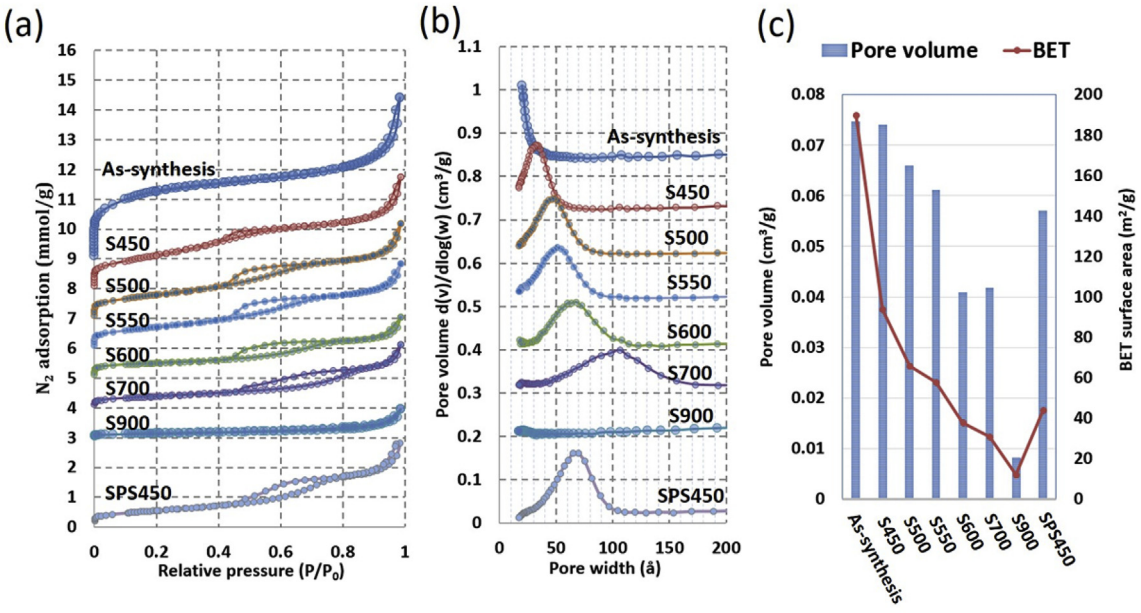

Fig. 5. a) N_2 adsorption-desorption isothermal curves measured at 77 K; b) Pore distribution calculated from the adsorption curve by BJH method; c) the volume of the pores in the sizes between 1.5 nm and 15 nm and the BET surface area. The baseline of each curve in a) and b) was adjusted to avoid overlapping.

coarsening (Fig. 6). The former one involves grain boundary diffuse, lattice diffuse and plastic flow causing the shrink of the particles. While the latter one is responsible for the formation of mesopores in this work. The sharp increase of the pore size after sintering indicates the strong coarsening effect took place during the sintering. The coarsening normally involves lattice diffusion (from the surface), the surface diffusion and vapor transportation [18,28]. We have previously observed the coalescence of ZrO_2 nanocrystals through sliding and rotating takes place during sintering at lower than normal sintering temperature [29]. In this study, aligned crystallites with the size of 3–5 nm in the as-synthesized aggregates facilitated the coalescence making it another possible mechanism contributing to the strong coarsening effect.

The porosity of the monolith sintered aggregate sample was also studied. Comparing to S450, the SPS450 sample shows around 20% less pore volume but around 100% larger average pore size. While comparing to S600, the SPS450 shows similar average pore size but around 40% larger pore volume. The differences are most likely due to the enhanced mass transportation during SPS process which strongly contributes more to the coarsening leading to a larger pore size than the counterpart from pressureless sintering.

The effect of mesopores on the thermal conductivity is investigated in this study. In order to measure the thermal conductive of the powders, pellets were fabricated by uniaxial die pressing of the as-synthesized YSZ powder mixed with 10 wt% binder and sintered at different temperatures ranging from 450 °C to 900 °C. Thermal gravimetric analysis was carried out and shows that the binder burns off at around 400 °C. Therefore all of the sintered samples are binder-free. Fig. 7 shows that, comparing to the macroporous YSZ from Ref.20–22, the mesoporous YSZ pellets sintered at 450 °C,

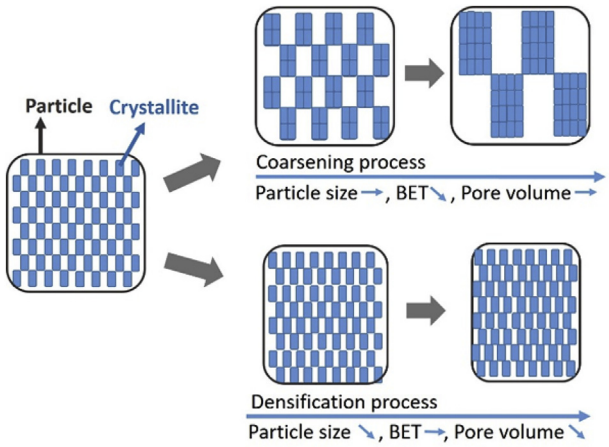

Fig. 6. Scheme of the development of the crystal arrangement in a particle during sintering.

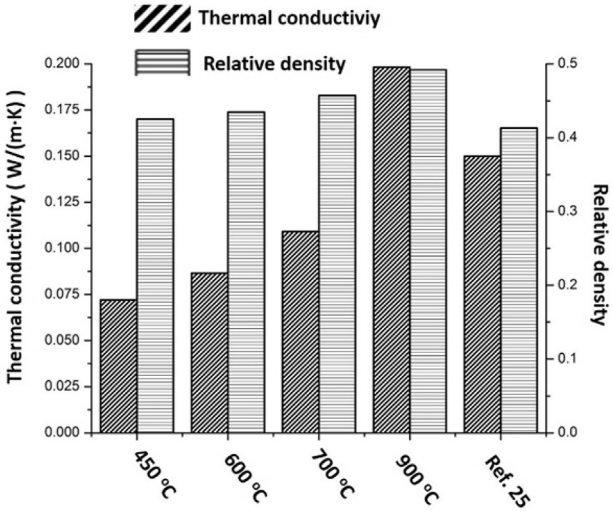

Fig. 7. Thermal conductivity and relative density of the mesoporous YSZ pellets sintered at different temperature.

600 °C and 700 °C show higher densities but considerably lower thermal conductivity. This indicates that with similar pore volume, mesopores are more effective than macropores to reduce the thermal conductivity. Increase the sintering temperature to 900 °C caused slightly increase of relative density, however, removed most of the mesopores in the materials thus led to the sharp increase of thermal conductivity. This also indicates the importance of the mesopores in reducing the thermal conductivity.

4. Conclusions

In summary we have shown that mesoporous YSZ self-supported mesocrystals with the tunable mesopore can be obtained through a chemi-thermal process starting with a hydrothermal synthesis followed by heat treatment. The heat treatment can be considered as a sintering process for each particle. Due to the microstructure features of the as-synthesized aggregates, the coarsening is enhanced and outweigh the densification mechanisms, resulting in the generation of the mesopores while maintaining considerable pore volume. As an example of the potential applications, we show that the mesoporous YSZ is an excellent thermal isolator with considerably lower thermal conductivity than its macroporous counterpart. This work not only provides a low cost and scalable method for preparing mesoporous YSZ self-supported mesocrystal powders, but also gives a new perspective for preparing a wide range of mesoporous inorganic oxide materials.

Author contributions

All authors have given approval to the final version of the manuscript.

Acknowledgment

Berzelii Center Exselent on Porous Materials was acknowledged for financial support to this work, so does the Swedish Research Council. We also thank JECS Trust for providing the travelling grant.

The microstructural characterization part of the work was performed at the Electron Microscopy Centre of Stockholm University, which is supported by the Knut and Alice Wallenberg Foundation and Electron Microscopy Center of University of Birmingham.

Abbreviations

YSZ	yttria stabilized zirconia
TEM	transmission electron microscopy
HR-TEM	high resolution transmission electron microscopy
SPS	spark plasma sintering
SAED	selected area electron diffraction

References

[1] Tartaj P, Amarilla JM. Multifunctional response of anatase nanostructures based on 25 nm mesocrystal-like porous assemblies. Adv Mater 2011;23:4904–7. https://doi.org/10.1002/adma.201103168.

[2] Zhou L, O'Brien P. Mesocrystals: a new class of solid materials. Small 2008;4:1566–74. https://doi.org/10.1002/smll.200800520.

[3] Yu Y, Zhang J, Wu X, Zhao W, Zhang B. Nanoporous single-crystal-like CdxZn1−xS nanosheets fabricated by the cation-exchange reaction of inorganic-organic hybrid ZnS-amine with cadmium ions. Angew Chem Int Ed 2012;51:897–900. https://doi.org/10.1002/anie.201105786.

[4] Bian Z, Zhu J, Wen J, Cao F, Huo Y, Qian X, et al. Single-Crystal-like titania mesocages. Angew Chem Int Ed 2011;50:1105–8. https://doi.org/10.1002/anie.201004972.

[5] Adachi * Motonari, Murata Yusuke, Takao Jun, Jiu Jinting, Sakamoto A Masaru, Wang F. Highly efficient dye-sensitized solar cells with a titania thin-film electrode composed of a network structure of single-crystal-like TiO2 nanowires made by the "oriented attachment" mechanism. J Am Chem Soc 2004;126:14943–9. https://doi.org/10.1021/JA048068S.

[6] Crossland EJW, Noel N, Sivaram V, Leijtens T, Alexander-Webber JA, Snaith HJ. Mesoporous TiO2 single crystals delivering enhanced mobility and optoelectronic device performance. Nature 2013;495:215–9.

[7] Bergström L, Sturm (née Rosseeva) EV, Salazar-Alvarez G, Cölfen H. Mesocrystals in biominerals and colloidal arrays. Acc Chem Res 2015;48:1391–402. https://doi.org/10.1021/ar500440b.

[8] Liu Y, Luo Y, Elzatahry AA, Luo W, Che R, Fan J, et al. Mesoporous TiO_2 mesocrystals: remarkable defects-induced crystallite-interface reactivity and their in situ conversion to single crystals. ACS Cent Sci 2015;1:400–8. https://doi.org/10.1021/acscentsci.5b00256.

[9] Das SK, Bhunia MK, Sinha AK, Bhaumik A. Self-Assembled mesoporous zirconia and sulfated zirconia nanoparticles synthesized by triblock copolymer as template. J Phys Chem C 2009;113:8918–23. https://doi.org/10.1021/jp9014096.

[10] Banerjee B, Bhunia S, Bhaumik A. Self-assembled sulfated zirconia nanocrystals with mesoscopic void space synthesized via ionic liquid as a porogen and its catalytic activity for the synthesis of biodiesels. Appl Catal Gen 2015;502:380–7. https://doi.org/10.1016/j.apcata.2015.06.028.

[11] Li Y, Liu L, Zou X, Hedin N, Gao F. Nanocrystalline TON-type zeolites synthesized under static conditions. Microporous Mesoporous Mater 2018;256:84–90. https://doi.org/10.1016/j.micromeso.2017.07.050.

[12] Fang Y, Hu H, Chen G. In situ assembly of zeolite nanocrystals into mesoporous aggregate with single-crystal-like morphology without secondary template. Chem Mater 2008;20:1670–2. https://doi.org/10.1021/cm703265q.

[13] Yin J, Gao F, Wei C, Lu Q. Water amount dependence on morphologies and properties of ZnO nanostructures in double-solvent system. Sci Rep 2014;4:3736.

[14] Zhou X, Wang G, Guo L, Chi H, Wang G, Zhang Q, et al. Hierarchically structured TiO_2 for Ba-filled skutterudite with enhanced thermoelectric performance. J Mater Chem 2014;2:20629–35. https://doi.org/10.1039/C4TA05285D.

[15] Wang Y, Price AD, Caruso F, Yano K, Ren N, Gao Z, et al. Nanoporous colloids: building blocks for a new generation of structured materials. J Mater Chem 2009;19:6451. https://doi.org/10.1039/b901742a.

[16] Gao F, Sougrat R, Albela B, Bonneviot L. Nanoblock Aggregation–Disaggregation of zeolite nanoparticles: temperature control on crystallinity. J Phys Chem C 2011;115:7285–91. https://doi.org/10.1021/jp111928j.

[17] Somiya S. Handbook of advanced ceramics : materials, applications, processing, and properties. n.d. 2013.

[18] German RM. Sintering theory and practice. Wiley; 1996.

[19] Chytil S, Haugland L, Blekkan EA. On the mechanical stability of mesoporous silica SBA-15. Microporous Mesoporous Mater 2008;111:134–42. https://doi.org/10.1016/j.micromeso.2007.07.020.

[20] Zhang H, Lu H, Zhu Y, Li F, Duan R, Zhang M, et al. Preparations and characterizations of new mesoporous ZrO2 and Y2O3-stabilized ZrO2 spherical powders. Powder Technol 2012;227:9–16. https://doi.org/10.1016/j.powtec.2012.02.007.

[21] Wang H, Chen H, Ni B, Wang K, He T, Wu Y, et al. Mesoporous ZrO_2 nanoframes for biomass upgrading. ACS Appl Mater Interfaces 2017;9:26897–906. https://doi.org/10.1021/acsami.7b07567.

[22] Hu L, Wang C-A, Huang Y. Porous yttria-stabilized zirconia ceramics with ultra-low thermal conductivity. J Mater Sci 2010;45:3242–6. https://doi.org/10.1007/s10853-010-4331-9.

[23] Schlichting KW, Padture NP, Klemens PG. Thermal conductivity of dense and porous yttria-stabilized zirconia. J Mater Sci 2001;36:3003–10. https://doi.org/10.1023/A:1017970924312.

[24] Nait-Ali B, Haberko K, Vesteghem H, Absi J, Smith DS. Thermal conductivity of highly porous zirconia. J Eur Ceram Soc 2006;26:3567–74. https://doi.org/10.1016/J.JEURCERAMSOC.2005.11.011.

[25] Deng Z-Y, Ferreira JMF, Tanaka Y, Isoda Y. Microstructure and thermal conductivity of porous ZrO2 ceramics. Acta Mater 2007;55:3663–9. https://doi.org/10.1016/J.ACTAMAT.2007.02.014.

[26] Ersen O, Florea I, Hirlimann C, Pham-Huu C. Exploring nanomaterials with 3D electron microscopy. Mater Today 2015;18:395–408. https://doi.org/10.1016/j.mattod.2015.04.004.

[27] Coleman SC, Beeré WB. The sintering of open and closed porosity in UO_2. Philos Mag A 1975;31:1403–13. https://doi.org/10.1080/00318087508228691.

[28] Kellett BJ, Lange FF. Thermodynamics of densification: I, sintering of simple particle arrays, equilibrium configurations, pore stability, and shrinkage. J Am Ceram Soc 1989;72:725–34. https://doi.org/10.1111/j.1151-2916.1989.tb06208.x.

[29] Kocjan A, Logar M, Shen Z. The agglomeration, coalescence and sliding of nanoparticles, leading to the rapid sintering of zirconia nanoceramics. Sci Rep 2017;7:2541. https://doi.org/10.1038/s41598-017-02760-7.

<au id="1">**Dr. Zhijian Shen** is a full professor in Department of Materials and Environmental Chemistry, Arrhenius Laboratory, Stockholm University, Sweden. He received his PhD degree in 1990 in China. His main research focus are on developing ceramics with novel or improved functions for demanded applications though exploring the potentials of advanced processes. To date, he has published about 200 scientific articles, has edited a book, and has filed more than 20 patents and patent applications.

<au id="2">**Dr. Leifeng Liu** is currently a research associate professor at South University of Science and Technology of China. He received his bachelor degree from Hunan University in 2007; master degree from Chinese Academy of Science in 2010 and PhD degree from Stockholm University in 2014. His primary scientific interests cover the field of the relationship between microstructure and properties of inorganic materials especially structural materials,